Structural Changes in the Mo(100) Reconstruction

R. S. Daley,[1] T. E. Felter,[1] M. L. Hildner,[1] and P. J. Estrup[2]
[1]*Sandia National Laboratories, Livermore, California 94550*
[2]*Brown University, Providence, Rhode Island 02912*
(Received 15 September 1992)

The clean Mo(100) surface reconstructs at low temperature forming a commensurate $c(7\sqrt{2}\times\sqrt{2})R45°$ displacement wave. LEED studies over the range 10 to 300 K reveal a change in the harmonic content of this wave at intermediate temperatures corresponding to a sharpening of antiphase domain walls as T is lowered. Simultaneously, a selection of one of two possible domain orientations occurs if steps are present. The process shows no hysteresis and permits the equilibrium distribution to be observed.

PACS numbers: 68.35.Bs, 68.35.Md, 68.35.Rh

Reconstructions of the clean (100) surfaces of Mo [1] and W [1,2] below room temperature have continued to present interesting experimental and theoretical problems since their discovery. While tungsten has received the greater attention in the large body of work that has evolved, the molybdenum surface provides a more challenging problem due to its complex reconstructed unit mesh. The intricate nature of the Mo structure is demonstrated by the fact that not until recently, from atom diffraction [3] and LEED [4] studies, has it become clear that the low-temperature structure—initially believed to be incommensurate—is actually high-order commensurate. Our LEED results have identified the unit mesh as $c(7\sqrt{2}\times\sqrt{2})R45°$, reminiscent of the (7×7) unit mesh in the well-known Si(111) reconstruction. In this Letter we discuss structural changes of this surface, observed by cooling the Mo crystal to liquid-He temperature; the data include unexpected results for the effect of temperature on the atomic geometry and on the selection of domain orientation.

In many respects the Mo reconstruction is similar to that of W for which there is now general agreement about the structure. In particular, the tungsten surface gives rise to a $(\frac{1}{2}\ \frac{1}{2})$ spot in the LEED pattern below room temperature which shows that the unit mesh is $(\sqrt{2}\times\sqrt{2})R45°$ [1,2] containing two surface atoms. It is also known that the reconstruction consists of W atom displacements in the surface plane along the ⟨11⟩ direction [5,6], of magnitude 0.24 Å [7–10], that second-layer displacements are about 5 times smaller [8], and that the reconstruction is a continuous phase transition with a critical temperature T_c near 220 K [11].

Although less extensive, detailed information is available also for Mo(100): T_c is around 150 K [12], the Mo atom displacements are in the ⟨11⟩ direction [13] and have magnitude 0.12 Å according to HEIS (high-energy ion scattering) [4], and adsorbed hydrogen modifies the reconstruction to produce a rich phase diagram [14]. The driving mechanism for the transition is being debated, and models using either short-range forces [15] or long-range interactions (via a Fermi surface instability) [16] have been proposed. In addition, progress has been made in formulating a realistic Mo-Mo potential [17].

Figure 1 shows the LEED pattern for the clean Mo(100) surface at 10 K. In addition to the normal (integer-order) spots the pattern contains extra features in $\frac{1}{7}$-order positions, the most prominent being those closest to the $(\frac{1}{2}\ \frac{1}{2})$ positions, giving the appearance of "split" half-order spots. In earlier work, only these two prominent spots were observed along with the second pair from the domain rotated by 90°, together producing a quartet of spots around $(\frac{1}{2}\ \frac{1}{2})$. The uncertainty in the degree of splitting in these earlier studies [1] led to the suggestion that the structure was incommensurate. In Fig. 1, one domain orientation dominates and since a row of four additional $\frac{1}{7}$-order spots are seen for this orientation, the reconstructed surface must be commensurate.

There are four space groups compatible with the centered rectangular Bravais lattice indicated by the LEED pattern: $p1$, $p2$, $c1m1$, and $c2mm$. The last has the highest symmetry and agrees with the point symmetries

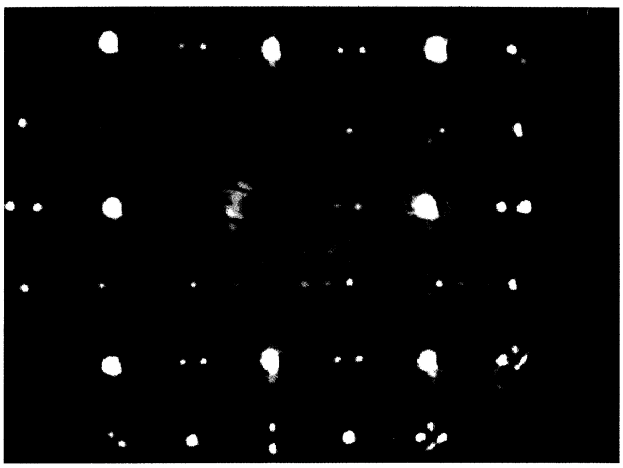

FIG. 1. LEED pattern of the reconstructed Mo(100) $c(7\sqrt{2}\times\sqrt{2})R45°$ surface at 10 K. Electron beam is at 156 eV, and normal incidence.

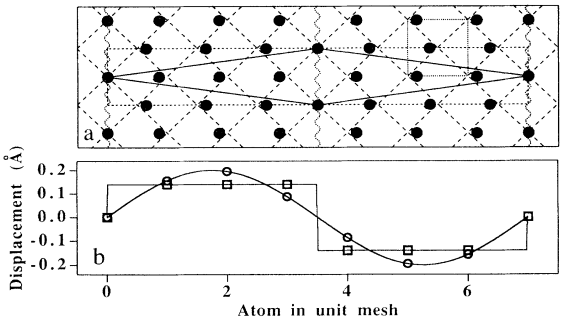

FIG. 2. (a) $c(7\sqrt{2}\times\sqrt{2})R45°$ antiphase domain model for the Mo(100) reconstruction. Displacements exaggerated for illustration (applies at $T < 125$ K). (b) Plot of displacements for periodic lattice distortion; PLD (circles) applies at 125 K $< T <$ 180 K, and APD (squares) at lower T.

found in the LEED pattern. Figure 2 depicts a model of the unit cell consistent with these observations: fourteen atoms in a centered rectangular cell (dashed lines), corresponding to seven atoms in the primitive rhombohedral cell (solid lines). In order to satisfy $c2mm$ symmetry, any displacement must be along ⟨11⟩, i.e., parallel to the rectangle. The components perpendicular to the surface are small [18] aside from a uniform relaxation of the top layer [4].

The displacement on the nth surface atom is a sum of sinusoidal waves:

$$\delta_n = \sum_j \mathbf{A}_j \sin(\mathbf{q}_j \cdot \mathbf{r}_n), \quad j = 1,2,3, \tag{1}$$

where δ_n and $\mathbf{r}_n$ are the vector displacement and the (undistorted) position, respectively. $\mathbf{A}_j$ is the (vector) amplitude of the jth component of the displacement wave with $\mathbf{q}_j = j\frac{3}{7}\mathbf{G}_{11}$ where $\mathbf{G}_{11}$ is the unit reciprocal vector ⟨11⟩. The longest period compatible with the unit cell (i.e., the fundamental) corresponds to $j = 1$.

Although precise values of δ_n are virtually unobtainable due to the large unit mesh, the relative intensities of the 6 extra beams reflect the Fourier composition of the structure. Careful measurements of these intensities as a function of temperature show that the *harmonic content changes with temperature*—a characteristic which to date is unique among high-order commensurate surface systems; neither the Si(111)(7×7) nor the Ge(111)c(2×8) surfaces show this behavior [19], for example, and for other likely candidates such as the reconstructed (100) surfaces of Au and Pt [20] rotational transformations dominate. The development of higher harmonics at low temperature has been observed, however, in 3D magnetic systems [21].

Figure 3(a) shows the intensity of the six fractional spots in the first reciprocal cell during cooling. The spots are labeled by single integers (see inset) and are symmetrically related in pairs at normal incidence. The 3 and 4 spots are the most intense. Below 125 K, the ranking of

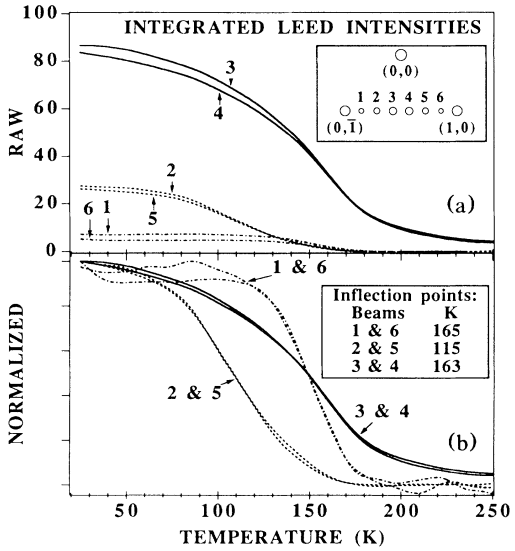

FIG. 3. (a) Fractional-order LEED intensities as a function of temperature. Incident beam energy, 46 eV. (b) As in (a), but normalized. Inset: Schematic of the first reciprocal mesh in the LEED pattern; note shorthand labeling convention.

the intensities is $I_{3,4} > I_{2,5} > I_{1,6}$ while at intermediate temperatures ($T \cong 150$ K), $I_{3,4} > I_{1,6} > I_{2,5}$. Figure 3(b) shows the normalized results. These data were obtained at a LEED energy of 46 eV but the behavior seen in Fig. 3(b) was found to be independent of electron energy. For $T > 175$ K and $T < 75$ K, the curves are rather "flat," increasing only slowly with cooling. In agreement with previous work [12], most of the intensity increase occurs in a relatively small temperature region; e.g., from 20% to 80% over an interval of less than 75 K, indicating a phase transition. We found that correcting the data by a Debye-Waller factor changed the intensity of the spots by only a few percent in the temperature interval covered in Fig. 3. This was expected since the Debye temperature of Mo is high.

The point of inflection in Fig. 3(b) (used as a measure of the critical temperature) is near 165 K for the 1, 3, 4, and 6 beams. For the 2 and 5 beams, however, the increase in intensity occurs at much lower temperature, showing that the geometry giving rise to these spots does not develop until ~50 K below the critical temperature of the phase transition. Thus, at these lower temperatures there is a further change in the structure, i.e., in the details of the atom displacements within the unit mesh. Since the positions of the spots and the symmetry of the LEED pattern do not change with temperature, the superstructures have the same $c(7\sqrt{2}\times\sqrt{2})R45°$ net; we therefore do not consider the final low-temperature structure to be a new phase.

It is instructive to consider two extreme models described by Eq. (1). The first of these, which we call a periodic lattice distortion, or PLD, corresponds to the

case where only a single Fourier component, the fundamental, describes the displacement pattern, i.e., $\{\mathbf{A}_j\} = \{\mathbf{A},0,0\}$. The corresponding structure factor then becomes [22]

$$S(\mathbf{k}) \propto \sum_n \exp[i\mathbf{k}\cdot(\mathbf{r}_n+\delta_n)]$$
$$= \sum_m i^{|m|}(-i)^m J_{|m|}(\mathbf{k}\cdot\mathbf{A}) \sum_n \exp[i(\mathbf{k}+m\mathbf{q})\cdot\mathbf{r}_n],$$

where J_m is the mth order Bessel function and $\mathbf{k}$ is the momentum transfer in the diffraction event. The maxima in $S(\mathbf{k})$ occur when $\mathbf{k}+m\mathbf{q}=\mathbf{G}$, where $\mathbf{G}$ is a reciprocal lattice vector of the undistorted surface. An accurate calculation of the corresponding LEED intensities would require a dynamical analysis. The large unit cell makes this very difficult but the kinematical structure factor can be expected to provide an acceptable estimate of the (energy independent) intensity ratios. Spots 3, 1, and 2 are produced for m values of 1, 2, and 3, respectively, with kinematic intensities proportional to $J_m^2 \cong (\mathbf{k}\cdot\mathbf{A})^{2m}$ (since $\mathbf{k}\cdot\mathbf{A}$ is small). Therefore, to lowest order in the kinematical approximation, the diffracted intensities for spots 3, 1, and 2 are proportional to $(\mathbf{k}_3\cdot\mathbf{A})^2$, $(\mathbf{k}_1\cdot\mathbf{A})^4$, and $(\mathbf{k}_2\cdot\mathbf{A})$ [6], respectively, in qualitative agreement with the experimental ranking at intermediate temperatures. Thus, the sinusoidal PLD approximates the structure in the intermediate temperature range. However, it fails at low temperature.

The second model is comprised of antiphase domains (APD) of $(\sqrt{2}\times\sqrt{2})R45°$, i.e., tungsten type reconstruction (Fig. 2, dotted lines), separated by domain walls. The walls are formed by the undisplaced atoms. In this case, Eq. (1) is solved under the constraints $\delta_0=0$, and $\delta_{1,2,3}=-\delta_{4,5,6}=\delta$ and leads to the amplitudes $\{\mathbf{A}_j\} = \{1.25\delta, -0.14\delta, 0.36\delta\}$. The first-order contributions to the intensity of the 3, 2, and 1 spots are $(\mathbf{k}_3\cdot\mathbf{A}_1)^2$, $(\mathbf{k}_2\cdot\mathbf{A}_3)^2$, and $(\mathbf{k}_1\cdot\mathbf{A}_2)^2$, respectively. The resulting ratios are 1.00:0.72:0.25 which agree with the experimental ranking at $T<125$ K. Thus, the low-temperature structure is well represented by a regular array of domain walls separating antiphase regions of $(\sqrt{2}\times\sqrt{2})R45°$.

The distinction between these two simplified models is most easily seen in Fig. 2(b). For the APD (squares) the displacements of the six atoms in the primitive unit mesh are of equal magnitude, three in one direction and three in the opposite direction, and the seventh is undisplaced. For the PLD (circles) the displacements follow a sine curve. The magnitudes of the displacement were determined for each model by fitting to ion scattering results [3].

Evidently, LEED is a discriminating tool for detecting rather subtle changes that occur as a function of temperature in the Mo reconstructed unit mesh. Although one expects the real system to lie somewhere in between the extreme versions of the PLD and APD, the fact that the reconstruction moves from a condition nearer to the PLD to one nearer to the APD during cooling seems physically

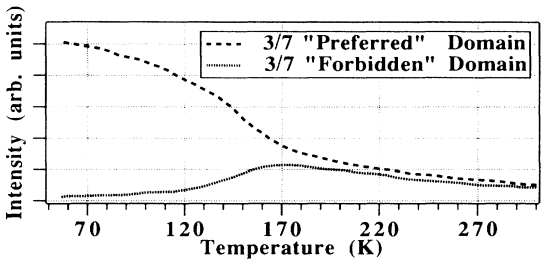

FIG. 4. Symmetry-related LEED intensities exhibit domain selection induced by steps. The large increase in intensity below T_c for the favored domain and the decrease for the suppressed domain is clearly seen.

reasonable. This can be thought of as a sharpening of the structure into well-defined $(\sqrt{2}\times\sqrt{2})R45°$ antiphase domains as T decreases. Equivalently it can be viewed as a thickening of the domain walls with increasing T; as the structure changes from APD to PLD, atoms near the domain walls become less displaced, i.e., they become more like domain wall atoms. These conclusions agree with predictions of recent molecular dynamics calculations [15] which assume that competing surface and bulk forces are responsible for the reconstruction. However, this model may need to be modified since it also predicts rather large perpendicular displacements at the domain walls, in contradiction to our LEED and HEIS data [18].

Another factor that can influence the relative LEED intensities is the distribution of domain widths resulting from meandering walls. While it is unnecessary to invoke such a domain distribution for the clean surface, we do find evidence for this in the case of mild contamination, which we believe pins domain walls so as to prevent the formation of straight, equally spaced structures. This, in turn, destroys spots 1, 2, 5, and 6 without strong attenuation of spots 3 and 4 since the average wall spacing is unchanged.

Intrinsic defects also affect the domain distribution and this influence can help reveal the nature of the phase transition. An interesting result attributable to steps is shown in Fig. 4. At "high" temperatures, $170\text{ K} < T < 300$ K, domains oriented along $\langle 11\rangle$ and $\langle 1\,-1\rangle$ are equally populated; thus, their intensities follow similar temperature behavior. As the critical temperature is reached, however, the intensities diverge. At the lowest temperatures, one domain orientation is entirely suppressed while the other dominates. The selection of one domain over the other occurs when the correlation length becomes comparable to the terrace width. Since the correlation length diverges at T_c and since the terrace width is rather large, this selection process occurs near T_c. Depending on the terrace orientations, one or the other domain or even coexistence can be achieved. In the domain selection process, hysteresis is absent, suggesting that the transition is second order. We wish to point out, however, that the evidence does not conclusively rule out

a (weak) first-order transition. Domain selection would then occur when the size of the islands of the low-T phase becomes comparable to the terrace width. A difficulty with the hypothesis of a first-order transition is that the initial nucleation would be expected to occur at step edges so that domain selection should be seen from the very beginning. It should also be noted that clean W(100) shows a qualitatively similar domain selection [23] and that in this case there is good evidence that the phase transition is continuous [11].

In summary, the low-temperature behavior of the clean reconstructed Mo(100) surface has been shown to be surprisingly complex. At $T_c \cong 165$ K the reconstruction develops long-range order with a $c(7\sqrt{2}\times\sqrt{2})R45°$ periodicity which persists upon further cooling. The precise location of the surface atoms is currently being studied by surface x-ray diffraction [24], and theoretical investigations of the structure are underway [25]. However, an unprecedented effect is observed with decreasing temperature: Within the unit cell a continuous change in atomic displacements occurs, resulting in a gradual sharpening of the antiphase domain walls. Changes occur simultaneously on a larger scale: While at $T \cong 200$ K the two possible directions of the displacement waves tend to occur with equal probability, at $T < T_c$ a lifting of the orientational degeneracy becomes observable.

This work was supported by the U.S. DOE, Office of Basic Energy Sciences, Division of Materials Science and by the National Science Foundation through Grant No. DMR-8615692. The expert technical assistance of B. V. Hess is gratefully acknowledged. R. H. Stulen is thanked for helpful discussions early on in this work. Recent discussions with G. Thomas, D. Chrzan, M. Daw, S. Foiles, D. Johnson, L. D. Roelofs, and S. C. Ying are greatly appreciated.

[1] T. E. Felter, R. A. Barker, and P. J. Estrup, Phys. Rev. Lett. **38**, 1138 (1977).
[2] M. K. Debe and D. A. King, J. Phys. C **10**, L303 (1977).
[3] D.-M. Smilgies and E. Hülpke, Phys. Rev. B **43**, 1260 (1991).
[4] M. L. Hildner, R. S. Daley, T. E. Felter, and P. J. Estrup, J. Vac. Sci. Technol. A **9**, 1604 (1991).
[5] M. K. Debe and D. A. King, Phys. Rev. Lett. **39**, 708 (1977).
[6] G.-C. Wang and T. M. Lu, Surf. Sci. **122**, L635 (1982).
[7] R. A. Barker, P. J. Estrup, F. Jona, and P. M. Marcus, Solid State Commun. **25**, 375 (1978).
[8] M. S. Altman, P. J. Estrup, and I. K. Robinson, Phys. Rev. B **38**, 5211 (1988).
[9] I. Stensgaard, L. C. Feldman, and P. J. Silverman, Phys. Rev. Lett. **42**, 247 (1979).
[10] J. A. Walker, M. K. Debe, and D. A. King, Surf. Sci. **104**, 405 (1981).
[11] I. K. Robinson, A. A. MacDowell, M. S. Altman, P. J. Estrup, K. Evans-Lutterodt, J. D. Brock, and R. J. Birgeneau, Phys. Rev. Lett. **62**, 1294 (1989).
[12] T. E. Felter, J. Vac. Sci. Technol. A **2**, 1008 (1984).
[13] R. A. Barker, S. Semancik, and P. J. Estrup, Surf. Sci. **94**, L162 (1980).
[14] J. A. Prybyla, P. J. Estrup, S. C. Ying, Y. J. Chabal, and S. B. Christman, Phys. Rev. Lett. **58**, 1877 (1987); J. A. Prybyla, P. J. Estrup, and Y. J. Chabal, J. Chem. Phys. **94**, 6274 (1991).
[15] C. Z. Wang, E. Tosatti, and A. Fasolino, Phys. Rev. Lett. **60**, 2661 (1988).
[16] K. E. Smith and S. D. Kevan, Phys. Rev. B **43**, 3986 (1991); X. W. Wang, C. T. Chan, and K.-M. Ho, Phys. Rev. Lett. **60**, 2066 (1988); E. Hülpke and D. M. Smilgies, Phys. Rev. B **40**, 1338 (1989); J. W. Chung, K. S. Shin, D. H. Balk, C. Y. Kim, H. W. Kim, S. K. Lee, C. Y. Park, S. C. Hong, T. Kinoshita, M. Watanabe, A. Kakizaki, and T. Ishii, Phys. Rev. Lett. **69**, 2228 (1992).
[17] J. A. Moriarty and R. Phillips, Phys. Rev. Lett. **66**, 3036 (1991).
[18] R. S. Daley, M. L. Hildner, T. E. Felter, L. Roelofs, and P. J. Estrup (unpublished).
[19] P. A. Bennett and M. B. Webb, Surf. Sci. **104**, 74 (1981); R. J. Phaneuf and M. B. Webb, Surf. Sci. **164**, 167 (1985).
[20] D. L. Abernathy, S. G. J. Mochrie, D. M. Zehner, G. Grübel, and D. Gibbs, Phys. Rev. B **45**, 9272 (1992).
[21] M. Habenschuss, C. Stassis, S. K. Sinha, H. W. Deckman, and F. H. Spedding, Phys. Rev. B **10**, 1020 (1974).
[22] R. W. James, *The Optical Principles of the Diffraction of X-Rays* (G. Bell, London, 1948).
[23] M. S. Altman, Ph.D. thesis, Brown University, 1989 (unpublished).
[24] D. M. Smilgies, P. J. Eng, and I. K. Robinson, preceding Letter, Phys. Rev. Lett. **70**, 1291 (1993).
[25] L. D. Roelofs and S. M. Foiles (to be published).

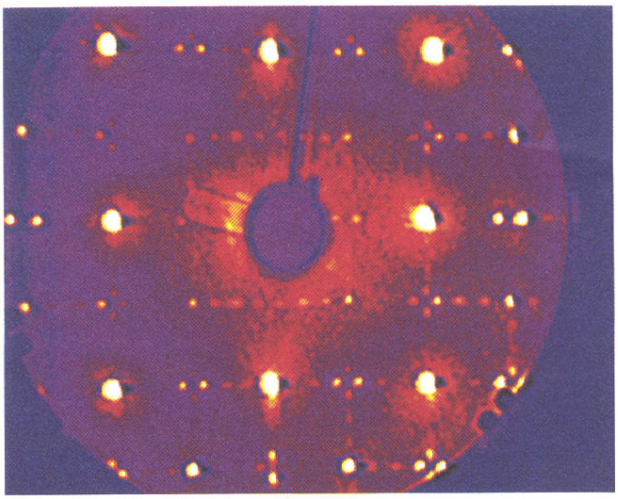

FIG. 1. LEED pattern of the reconstructed Mo(100) $c(7\sqrt{2}\times\sqrt{2})R45°$ surface at 10 K. Electron beam is at 156 eV, and normal incidence.